DISCRETE AND CONTINUOUS
DYNAMICAL SYSTEMS
SUPPLEMENT 2007

Website: www.AIMSciences.org

pp. **436–445**

TURING PATTERNS ON GROWING SPHERES: THE EXPONENTIAL CASE

Julijana Gjorgjieva

DAMTP
Centre for Mathematical Sciences
Wilberforce Road
Cambridge CB3 0WA, UK

Jon Jacobsen

Harvey Mudd College
Mathematics Department
301 Platt Blvd
Claremont, CA 91711, USA

Abstract. We consider Turing patterns for reaction-diffusion systems on the surface of a growing sphere. In particular, we are interested in the effect of dynamic growth on the pattern formation. We consider exponential isotropic growth of the sphere and perform a linear stability analysis and compare the results with numerical simulations.

1. **Introduction.** The formation and development of pattern and shape in biology is an interesting phenomenon known as *morphogenesis*. Any pattern or shape observed in nature, even though governed by genetics, is most likely produced by an unknown mechanism. Thus, determining these mechanisms that generate pattern and shape in organisms is an important goal of theoretical biologists. Of interest are mammalian coat patterns, seashell pigmentation patterns and tropical fish surface patterns, as well as any symmetry-breaking events: branching processes in plants, initiation of single or multiple new organs in animals, and solid tumor growth. One class of possible models for these processes of pattern formation are *reaction-diffusion systems* of the form

$$u_t = d\,\Delta u + f(\gamma, u), \tag{1}$$

for $d > 0$ and $\gamma \in \mathbb{R}$.

Reaction-diffusion models are particularly compelling with regard to their ability to capture complex evolving patterns. Equations such as (1) are surprisingly complex to analyze, largely due to their blending of local (diffusion) and global (reaction) phenomena. One can intuitively see pattern formation as the result of a competition between reaction (creating spikes in concentration) and diffusion (smoothing out gradients in concentration).

The application of reaction-diffusion equations to model pattern formation in biology was introduced by Turing [15], who suggested that a system of reacting and diffusing chemicals (*morphogens*) can interact to produce stable patterns in concentration (*Turing patterns*). Recent interest has focused on incorporating other

2000 *Mathematics Subject Classification.* Primary: 35K57; Secondary: 37N25, 92C15.
Key words and phrases. pattern formation, Turing, reaction-diffusion, sphere, growth.

biologically relevant features such as domain growth, shape, and curvature into the models. The role of domain growth in reaction-diffusion models was first studied by Newman and Frisch [13] in their studies of chick limb development. More recently Kondo and Asai [9] demonstrated that growth could account for the stripe patterning observed in the *Pomacanthus* fish, where new stripes are inserted as the fish ages (see also Painter et al. [12]). This work was extended by Crampin et al. [3, 4, 5, 6] in one-dimension, and Chaplain et al. [2], in two-dimensions, in the context of spherical tumor growth. In their work they also consider geometric effects such as the curvature of the sphere. Studies of geometric effects in reaction-diffusion equations have also been considered for spheres without growth [16], for domains where patterns develop with pentagonal symmetries [1], patterns on lady bugs [10], and whorl formation in the unicellular seaweed *Acetabularia acetabulum* [8].

Recently, Plaza et al. [14] developed a mathematical framework to consider general geometric and temporal dynamics for any surface defined by a regular parametrization. Given such a parametrization for the (possibly growing) surface $X(r,s,t) = (x(r,s,t), y(r,s,t), z(r,s,t))$, if $h_1 = |X_r|$ and $h_2 = |X_s|$ (i.e., the magnitude of the vectors defined by the indicated partial derivative of X), then the reaction-diffusion equation (1) becomes

$$u_t = \frac{d}{h_1 h_2}\left[\left(\frac{h_2}{h_1}u_r\right)_r + \left(\frac{h_1}{h_2}u_s\right)_s\right] - \left[\ln h_1 h_2\right]_t u + f(\gamma, u), \tag{2}$$

where $u = u(X(r,s,t),t)$. With growth and shape the diffusion is now anisotropic (with directional preference depending on the ratios h_2/h_1 and h_1/h_2) and the effective diffusion rate is rescaled by the product $h_1 h_2$. The equation (2) also has a new sink term depending on the time derivative of the product $h_1 h_2$. The parametrization approach allows one to model the curvature and time variations on a fixed computational domain.

In this note we apply the framework of [14] to consider the particular case of a reaction-diffusion system on an isotropically growing sphere with the growth function $\rho(t)$. With the parametrization

$$X(r,s,t) = \rho(t)\begin{pmatrix}\sin(\pi s)\cos(2\pi r)\\ \sin(\pi s)\sin(2\pi r)\\ \cos(\pi s)\end{pmatrix}, \tag{3}$$

for $r, s \in (0,1)$ the Laplacian term in (2) takes the form of the spherical Laplacian

$$\Delta_* u = \frac{1}{\pi^2}u_{ss} + \frac{1}{4\pi^2\sin^2(\pi s)}u_{rr} + \frac{\cos(\pi s)}{\pi\sin(\pi s)}u_s, \tag{4}$$

for $r, s \in (0,1)$. Therefore, the dimensionless form of a coupled system of reaction-diffusion equations on the surface of a sphere is modeled by the system:

$$u_t = \frac{1}{\rho^2}\Delta_* u - 2\frac{\dot\rho}{\rho}u + f(\gamma, u, v), \tag{5}$$

$$v_t = \frac{d}{\rho^2}\Delta_* v - 2\frac{\dot\rho}{\rho}v + g(\gamma, u, v), \tag{6}$$

for $r, s \in (0,1)$ and $t \geq 0$. The system is completed with periodic boundary conditions for r and s. However, due to the singular nature as $s \to 0$ or $s \to 1$, for computations we restrict $s \in (\varepsilon, 1-\varepsilon)$ and use Neumann boundary conditions for s. This corresponds to cropping off a tiny piece at each pole on the sphere.

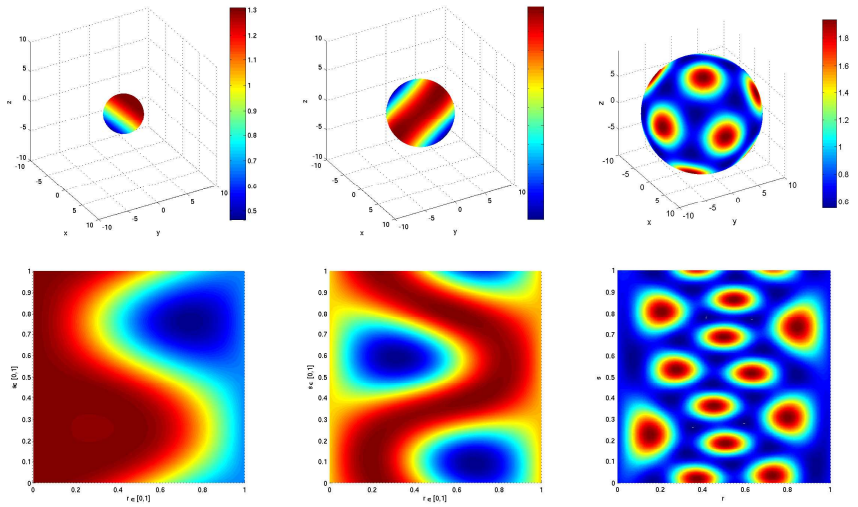

FIGURE 1. Patterns on a sphere of radius 3, 5, and 10 when the system (5)–(6) is solved with Schnakenberg kinetics $f(u,v) = a - u + u^2 v$ and $g(u,v) = b - u^2 v$ with $a = 0.07$ and $b = 0.95$. The top row images are the parametric images of the computational domain shown in the bottom row.

Figure 1 offers an example of the pattern on the surface of fixed spheres of radii 3, 5 and 10. Through the parametrization (3) one can imagine mapping the patterns of each computational domain shown in the bottom row of Figure 1 onto the surface of the corresponding sphere shown in the top row of Figure 1.

The introduction of time dependent coefficients in the model makes a full linear stability analysis for a growing sphere a challenging task. Accordingly, for this note we will restrict our attention to the case of exponentially growing spheres, where general conditions for Turing pattern formation can be derived. That is, in contrast to studying patterns on fixed spheres with different radii as a model for growing spheres, we consider the dynamic change of the spheres' radii by incorporating growth. In addition to being mathematically tractable, exponential and logistic growth are important and frequently encountered types of growth in biological systems.

2. **Exponentially Growing Spheres.**

In this section we perform a linear stability analysis for the reaction-diffusion system (5)-(6) on an exponentially growing sphere. We derive a set of conditions for pattern formation that extend the classical conditions for Turing patterns in the case of no growth (see e.g. [11]).

If we assume an exponentially growing sphere with a growth function $\rho(t) = e^{rt}$, then system (5)–(6) admits a spatially uniform equilibrium solution (u_0, v_0) defined by the system of equations

$$0 = \gamma f(u,v) - 2ru, \tag{7}$$

$$0 = \gamma g(u,v) - 2rv. \tag{8}$$

For the stability of this spatially uniform solution we consider a perturbation of the form

$$\mathbf{w}(t) = \begin{pmatrix} u(t) - u_0 \\ v(t) - v_0 \end{pmatrix}. \tag{9}$$

The linearized system governing the dynamics of $\mathbf{w}$ is defined by

$$\mathbf{w}_t = \gamma A\mathbf{w} - 2r\mathbf{w}, \tag{10}$$

where the stability matrix is given by

$$A = \begin{pmatrix} f_u & f_v \\ g_u & g_v \end{pmatrix}_{(u_0,v_0)}. \tag{11}$$

The solution $\mathbf{w}$ is linearly stable if all solutions of (10) of the form $\mathbf{w} = \mathbf{v}e^{\lambda t}$, have the property that $\mathrm{Re}(\lambda) < 0$. Substitution yields

$$\begin{aligned} \lambda\mathbf{v} &= \gamma A\mathbf{v} - 2r\mathbf{v} \\ &= \tilde{A}\mathbf{v}, \end{aligned}$$

where $\tilde{A} = \gamma A - 2rI$. The eigenvalues of $\tilde{A}$ are determined by

$$\begin{aligned} \det(\tilde{A} - \lambda I) &= \det\left(\gamma A - (2r + \lambda)\, I\right) \\ &= \left| \begin{pmatrix} \gamma f_u - 2r - \lambda & \gamma f_v \\ \gamma g_u & \gamma g_v - 2r - \lambda \end{pmatrix} \right| \\ &= 0. \end{aligned}$$

The resulting quadratic equation for λ is

$$\lambda^2 - \lambda\left(\gamma g_v + \gamma f_u - 4r\right) - 2r\gamma(f_u + g_v) + \gamma^2(f_u g_v - f_v g_u) + 4r^2 = 0, \tag{12}$$

which has solutions

$$\begin{aligned} \lambda_{1,2} =& \frac{1}{2}\left[(\gamma g_v + \gamma f_u - 4r)\right] \\ &\pm \frac{1}{2}\left[\left(\gamma g_v + \gamma f_u - 4r\right)^2 + 8r\gamma(f_u + g_v) - 4\gamma^2(f_u g_v - f_v g_u) - 16r^2\right]^{1/2}. \end{aligned} \tag{13}$$

Therefore, in the absence of diffusion the homogeneous solution (u_0, v_0) is stable when $\mathrm{Re}(\lambda) < 0$ for all λ, which will be true if

$$\mathrm{tr}\tilde{A} = \gamma(f_u + g_v) - 4r < 0, \tag{14}$$

$$\det\tilde{A} = \gamma^2(f_u g_v - f_v g_u) - 2r\gamma(f_u + g_v) + 4r^2 > 0. \tag{15}$$

These conditions generalize the classic conditions for the case of fixed domains which correspond to (14)–(15) when $r = 0$. In this case, the addition of the term $4r$ on the left-hand side in equation (14) allows the term $\gamma(f_u + g_v)$ to be small and positive while still maintaining validity, while for fixed domains (when $r = 0$) the term $\gamma(f_u + g_v)$ mush always be negative. This implies a larger set of parameter values for growing spheres for which the homogeneous solution is stable. For $r > 0$, condition (15) can be expressed as

$$\gamma^2(f_u g_v - f_v g_u) > 2r\left[\gamma(f_u + g_v) - 4r\right] = 2r\,\mathrm{tr}\tilde{A}. \tag{16}$$

Since $\mathrm{tr}\tilde{A} < 0$ by (14) this also implies a larger parameter set for linear stability of the homogeneous solution for fixed domains.

Next we consider conditions for a diffusion-driven instability. If we linearize about the steady state (u_0, v_0), the system (5)–(6) locally becomes

$$\mathbf{w}_t = \gamma A\mathbf{w} + D\Delta_*\mathbf{w} - 2r\mathbf{w}, \tag{17}$$

where A is the stability matrix (11), Δ_* is the spherical Laplacian (4), and D is the time-dependent diffusion matrix

$$D = \frac{1}{\rho^2}\begin{pmatrix} 1 & 0 \\ 0 & d \end{pmatrix} = \frac{1}{e^{2rt}}\begin{pmatrix} 1 & 0 \\ 0 & d \end{pmatrix}. \tag{18}$$

We consider spatially inhomogeneous solutions to (17) of the form

$$\mathbf{w}(\mathbf{x}, t) = \sum_k c_k e^{\lambda t}\mathbf{Y}_k(\mathbf{x}), \tag{19}$$

where $\mathbf{Y}_k$ are the spherical harmonics, and c_k are the Fourier coefficients obtained from the initial conditions. Substitution into (17) yields

$$\lambda\mathbf{Y}_k = \gamma A\mathbf{Y}_k - Dk^2\mathbf{Y}_k - 2r\mathbf{Y}_k.$$

The solution $\mathbf{Y}_k$ is nontrivial if the eigenvalues λ are roots to the characteristic polynomial

$$\det(\lambda I - \gamma A + Dk^2 + 2rI) = 0.$$

This determinant gives the quadratic polynomial for λ,

$$\lambda^2 + \left[e^{2rt}\left(k^2(1+d)e^{-2rt} - \gamma(f_u + g_v) + 4r\right)\right]\lambda + h(k^2) = 0, \tag{20}$$

whose constant term is quadratic in k^2, namely

$$\begin{aligned} h(k^2) =& de^{-4rt}(k^2)^2 - e^{-2rt}\left(\gamma(df_u + g_v) - 2r(1+d)\right)k^2 \\ &+ \gamma^2|A| - 2r\gamma(f_u + g_v) + 4r^2, \end{aligned} \tag{21}$$

and whose solutions are the eigenvalues $\lambda(k^2)$, as functions of the wavenumbers k^2. Notice that if $k^2 = 0$, we obtain conditions (14)–(15) for stability of the linearized system in the absence of spatial effects.

Here we are concerned with the conditions for instability in the presence of the diffusion. Therefore, the requirement for spatial instability is $\mathrm{Re}(\lambda) > 0$ for some $k^2 \neq 0$. Recall that the sum of the roots of a quadratic polynomial is the negative of the coefficient of the linear term, and the product of the roots is the constant term. Thus, $\mathrm{Re}(\lambda) > 0$ if the coefficient of λ is negative, or, if the free term $h(k^2)$ is negative for some $k^2 \neq 0$. The first part of the coefficient of the linear term is positive, i.e., $k^2(1+d) > 0$. The second part of the coefficient is also positive, by the first condition (14), established by ensuring stability of the homogeneous solution in the absence of diffusion, i.e., $-\gamma(f_u + g_v) + 4r > 0$. Therefore the coefficient in front of λ is positive, implying that for all values of k^2 the sum of the eigenvalues is negative. Hence, for an instability to occur, the constant term $h(k^2)$ in (21) must be negative. From the second condition for stability of the homogeneous steady state (15), it follows that the constant term in $h(k^2)$ is positive, and since $dk^4 > 0$, it follows that the coefficient in front of k^2 must be negative, namely

$$\gamma(df_u + g_v) - 2r(1+d) > 0. \tag{22}$$

This is the third condition for Turing pattern formation. From the conditions for stability in the absence of diffusion (14)–(15), it follows that $d \neq 1$, as is also the case for fixed domains [11].

Assuming that $h(k^2) < 0$ for some $k^2 \neq 0$, in order to achieve a diffusion-driven instability, we need the minimum value of $h(k^2)$, i.e., $h_{\min}$, to be negative. Letting $p = k^2$,

$$\begin{aligned} h(p) =& dp^2 e^{-4rt} - pe^{-2rt}\left(\gamma(df_u + g_v) - 2r(1+d)\right) \\ &+ \gamma^2|A| - 2r\gamma(f_u + g_v) + 4r^2. \end{aligned} \tag{23}$$

To find the minimum, we take the derivative

$$h'(p) = 2dpe^{-4rt} - e^{-2rt}\gamma[(df_u + g_v) - 2r(1+d)] = 0, \tag{24}$$

which has the solution

$$p = \frac{\gamma}{2d}e^{2rt}(df_u + g_v) + re^{2rt}\frac{1+d}{d}. \tag{25}$$

This is a minimum since $h''(p) = 2d > 0$. Therefore the critical k_m^2 for which $h(k^2)$ achieves a minimum is

$$k_m^2 = \frac{\gamma}{2d}e^{2rt}(df_u + g_v) + re^{2rt}\frac{1+d}{d}. \tag{26}$$

The value of h for this k^2 is

$$\begin{aligned} h_{\min} =& -e^{-4rt}\frac{\gamma^2}{4d}(df_u + g_v)^2 + e^{-4rt}r^2\left[3\frac{(1+d)^2}{d} + 4\right] \\ &+ \gamma re^{-4rt}\left[(df_u + g_v)\frac{1+d}{d} - 2(f_u + g_v)\right] + \gamma^2 e^{-4rt}|A|. \end{aligned} \tag{27}$$

To satisfy $h(k^2) < 0$, the condition

$$\begin{aligned} r^2\left[3\frac{(1+d)^2}{d} + 4\right] + \gamma r\left[(df_u + g_v)\frac{1+d}{d} - 2(f_u + g_v)\right] \\ + \gamma^2|A| < \frac{\gamma^2}{4d}(df_u + g_v)^2, \end{aligned} \tag{28}$$

must hold. This is the fourth condition for a Turing instability. Compared to the analogous expression without growth (when $r = 0$), the fourth condition for a Turing instability is significantly more complicated due to the addition of the linear and quadratic terms in r.

A bifurcation occurs when $h_{\min} = 0$, and in this example it happens when

$$\begin{aligned} r^2\left[3\frac{(1+d)^2}{d} + 4\right] + \gamma r\left[(df_u + g_v)\frac{1+d}{d} - 2(f_u + g_v)\right] \\ + \gamma^2|A| = \frac{\gamma^2}{4d}(df_u + g_v)^2. \end{aligned} \tag{29}$$

The critical diffusion coefficient ratio d_c is a solution to (29) for fixed kinetics parameters. The critical wavenumber for which a bifurcation occurs is

$$k_c^2 = \frac{\gamma}{2d_c}(d_c f_u + g_v) + r\frac{1+d_c}{d_c}. \tag{30}$$

Conditions (14)–(15), (22) and (28) are necessary, but not sufficient conditions for a Turing instability to occur. Even if all four conditions are satisfied, there will have to be an actual eigenmode in the unstable range. The range of wavenumbers k^2 such that $h(k^2) < 0$ can be determined from the range for which (20) has a

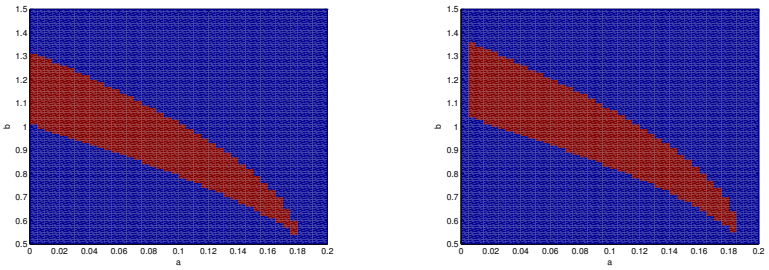

FIGURE 2. Example of Turing set for Schnakenberg kinetics as parameters a and b vary while keeping $d = 10$, for a fixed domain (left) and a growing domain (right) with $\rho(t) = e^{0.01t}$. Red indicates that a pattern can develop, while blue indicates it can not.

positive solution λ. For $d > d_c$ the range of unstable modes, $k_1^2 < k^2 < k_2^2$ is as follows:

$$\begin{aligned} k_1^2 =& \frac{e^{2rt}}{2d}\left[\gamma(df_u + g_v) - 2r(1+d)\right] \\ &- \frac{e^{2rt}}{2d}\sqrt{\left[\gamma(df_u + g_v) - 2r(1+d)\right]^2 - 4d\left[\gamma^2|A| - 2\gamma r(f_u + g_v) + 4r^2\right]}, \end{aligned} \tag{31}$$

and

$$\begin{aligned} k_2^2 =& \frac{e^{2rt}}{2d}\left[\gamma(df_u + g_v) - 2r(1+d)\right] \\ &+ \frac{e^{2rt}}{2d}\sqrt{\left[\gamma(df_u + g_v) - 2r(1+d)\right]^2 - 4d\left[\gamma^2|A| - 2\gamma r(f_u + g_v) + 4r^2\right]}. \end{aligned} \tag{32}$$

To summarize, the four conditions for the generation of spatial patterns by a two-species reaction-diffusion mechanism on an exponentially growing sphere are

$$\gamma(f_u + g_v) - 4r < 0, \tag{33}$$

$$\gamma^2(f_u g_v - f_v g_u) - 2r\gamma(f_u + g_v) + 4r^2 > 0, \tag{34}$$

$$\gamma(df_u + g_v) - 2r(1+d) > 0, \tag{35}$$

$$\begin{aligned} r^2\left[3\frac{(1+d)^2}{d} + 4\right] + \gamma r\left[(df_u + g_v)\frac{1+d}{d} - 2(f_u + g_v)\right] \\ + \gamma^2|A| - \frac{\gamma^2}{4d}(df_u + g_v)^2 < 0 \end{aligned} \tag{36}$$

Although analytically hard to compare with the fixed domain conditions, it is relatively straightforward to numerically check these conditions and pictorially display the set of Turing space where the conditions are satisfied for various reaction kinetics. In Figure 2 we show the two corresponding sets of Turing space for a fixed (left) and a growing sphere (right) with $\rho(t) = e^{0.01t}$. Notice that the region where conditions for pattern formation are satisfied (colored red) is shifted slightly upwards for the growing domain, implying that different values of the system produce a pattern in the cases of no growth versus exponential growth.

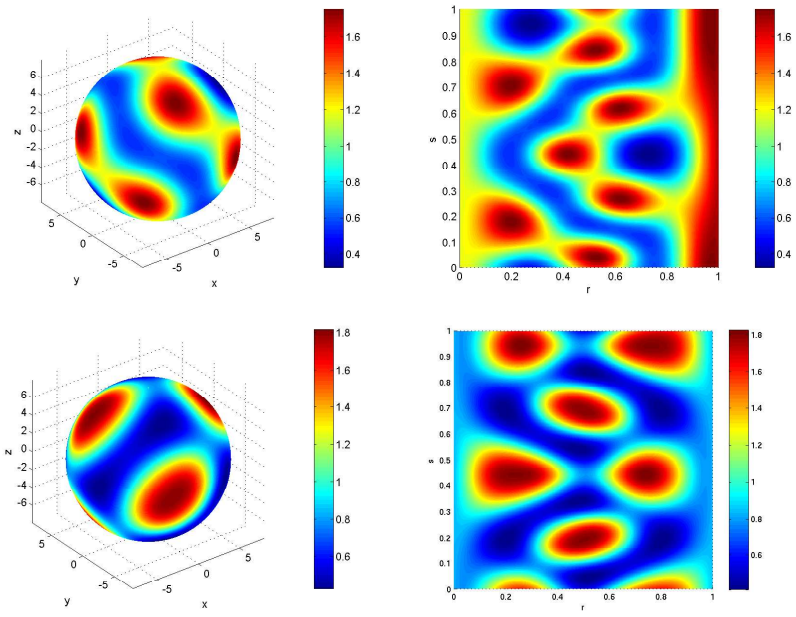

FIGURE 3. A comparison of the pattern on a fixed sphere of radius 8, with the pattern on a sphere exponentially growing from radius 4 to 8. Note that the growing sphere has a lower mode pattern.

3. **Numerical Results.** In this section we consider the previous results from a numerical point of view. In particular, we explore the difference between patterns for fixed spheres in contrast with the exponentially growing spheres.

Typically, with moderately fast growth, the pattern observed on the sphere's surface is of a lower mode than that of the fixed sphere of the same size. For example, Figure 3 shows the pattern simulated on the surface of a fixed sphere of radius 8 with the pattern on an exponentially growing sphere, which grows from a sphere of radius 4 to a sphere of radius 8, using the growth function $\rho(t) = 3+e^{0.01t}$. For easier comparison between the number of spots on each sphere, we show both the patterns on the surface of the sphere and on the computational domain. The fixed sphere of radius 8 exhibits a pattern with 8 spots and has a dominant eigenmode $k^2 = 30$. The sphere growing from radius 4 to radius 8 exhibits a pattern with 6 spots and has a dominant eigenmode $k^2 = 20$. This is the pattern which develops on a fixed sphere of radius 7 with all other conditions equal.

One way to understand this difference is to compare the Turing conditions for the fixed sphere and the growing sphere. Here we consider plots of the maxima of the real parts of λ versus the eigenmodes k^2 according to equation (20) for a growing sphere, and compare with the range of eigenmodes for which a pattern evolves for a fixed sphere of radius R. For instance, Figure 4 (left) shows the three-dimensional continuum of 10 such plots representing ranges for spheres of fixed radii $1, 2, \ldots, 10$. The figure for growing spheres looks similar. We consider spheres of radii 1, 2, 3, ..., 10. For a given growth rate we determine the time t^* at which the growing sphere attains the predetermined radius R, and for each time t^*, the range of unstable eigenmodes can be plotted as in Figure 4 (left).

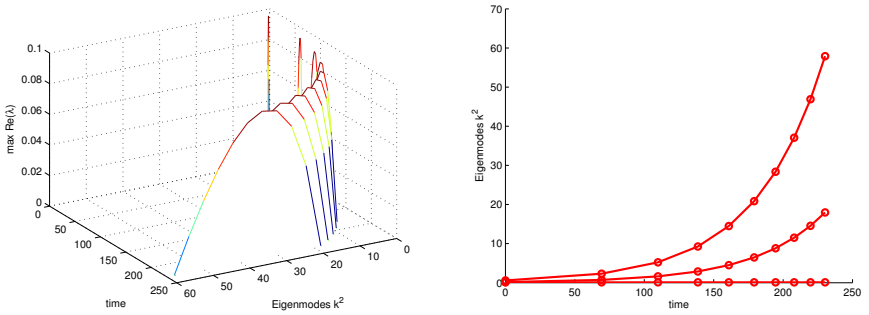

FIGURE 4. (i) A three-dimensional plot of the unstable eigenmode ranges for fixed spheres of radii $1, 2, \ldots, 10$. (ii) Top view of the unstable eigenmode ranges.

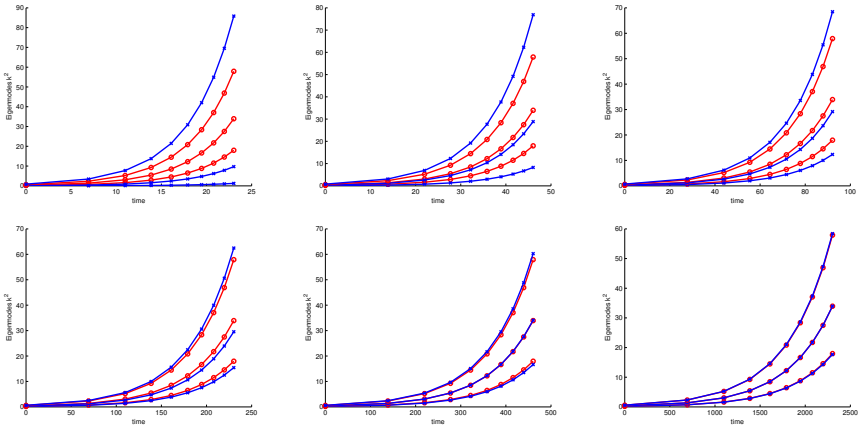

FIGURE 5. The range of unstable eigenmodes for fixed spheres (red/circles) and growing spheres (blue/crosses) growing spheres with $\rho(t) = e^{rt}$ for $r = 0.1, 0.05, 0.025, 0.01, 0.005$, and 0.001.

The result of this calculation is shown in Figure 5 where we display the top view of the eigenmodes ranges for fixed spheres of radii $1, 2, \ldots, 10$ for six different exponential growth functions. Note that in general, the range of eigenmodes which yield Turing pattern formation for a growing sphere is larger than the range for a fixed sphere, which implies that growth increases the number of possible patterns. However, the dominant eigenmode determining the pattern is smaller for growing spheres, in accordance with observations from numerical simulations, as in Figure 3. This phenomenon was consistently observed in our numerical simulations. Notice also from the figure, that only in the case of slow exponential growth can a growing sphere be modeled accurately by a continuum of fixed spheres. This shows that, although a larger class of patterns is allowed for growing spheres, a lower mode is typically selected. As the domain continues to grow there is the possibility of subsequent changes in the pattern from a bifurcation from a nonhomogeneous solution rather than a constant solution. We are currently analyzing this problem [7].

Acknowledgements. We would like to thank Pablo Padilla, Natalya St. Clair, and Jeff Hellrung. This work was supported in part by the W. M. Keck Foundation.

REFERENCES

[1] J. L. Aragón, M. Torres, D. Gil, R. A. Barrio and P. K. Maini, *Turing patterns with pentagonal symmetry*, Phys. Rev. E, **65** (2002), 1–9.

[2] M. A. J. Chaplain, M. Ganesh and I. G. Graham, *Spatio-temporal pattern formation on spherical surfaces: numerical simulation and application to solid tumour growth*, J. Math. Biol., **42** (2001), 387–423.

[3] E. J. Crampin, E. A. Gaffney and P. K. Maini, *Reaction and diffusion on growing domains: scenarios for robust pattern formation*, Bull. of Math. Biol., **61** (1999), 1093–1120.

[4] E. J. Crampin, E. A. Gaffney and P. K. Maini, *Mode-doubling and tripling in reaction-diffusion patterns on growing domains: a piecewise linear model*, J. Math. Biol., **44** (2002), 107–128.

[5] E. J. Crampin and P. K. Maini, *Modelling biological pattern formation: the role of domain growth*, Comments in Theoretical Biology, **6** (2001), 229-249.

[6] E. J. Crampin, W. W. Hackborn and P. K. Maini, *Pattern formation in reaction-diffusion models with nonuniform domain growth*, Bull. of Math. Biol., **64** (2002), 747–769.

[7] J. Gjorgjieva and J. Jacobsen, *Turing patterns on spheres*, in preparation.

[8] L. G. Harrison, S. Wehner and D. M. Holloway, *Complex morphogenesis of surfaces: theory and experiment on coupling of reaction-diffusion patterning to growth*, Faraday Discuss., **120** (2002), 277–293.

[9] S. Kondo and R. Asai, *A reaction-diffusion wave on the skin of the marine angelfish Pomacanthus*, Nature, **376** (1995), 765–768.

[10] S. S. Liaw, C. C. Yang, R. T. Liu and J. T. Hong, *Turing model for the patterns of lady beetles*, Phys. Rev. E, **64** (2001), 041909.1–5.

[11] J. D. Murray, "Mathematical Biology, II: Spatial Models and Biomedical Applications," 3rd ed., Springer-Verlag, New York, 2003.

[12] K. J. Painter, P. K. Maini and H. G. Othmer, *Stripe formation in juvenile Pomacanthus explained by a generalized Turing mechanism with chemotaxis*, Proc. Natl. Acad. Sci. USA, **96** (1996), 5549–5554.

[13] S. A. Newman and H. L. Frisch, *Dynamics of skeletal pattern formation in developing chick limb*, Science, (4407) **205** (1979), 662 - 668.

[14] R. G. Plaza, F. Sánchez-Garduño, P. Padilla, R. A. Barrio and P. K. Maini, *The effect of growth and curvature on pattern formation*, J. Dynam. Differential Equations, **16** (2004), 1093–1121.

[15] A. M. Turing, *The chemical basis of morphogenesis*, Philos. Trans. R. Soc. Lond. B, **237** (1952), 37–72.

[16] C. Varea and J. L. Aragón, J. L. and R. A. Barrio, *Turing patterns on a sphere*, Phys. Rev. E, **60** (1999), 4588–4592.

Received September 2006; revised April 2007.

E-mail address: julegjor@gmail.com
E-mail address: jacobsen@math.hmc.edu